PCCP

Cite this: *Phys. Chem. Chem. Phys.*, 2012, **14**, 8620–8627

www.rsc.org/pccp

PAPER

Efficiency enhancement in dye sensitized solar cells using gel polymer electrolytes based on a tetrahexylammonium iodide and MgI_2 binary iodide system

T. M. W. J. Bandara,*[ab] M. A. K. L. Dissanayake,[c] W. J. M. J. S. R. Jayasundara,[d] I. Albinsson[e] and B.-E. Mellander[a]

Received 29th December 2011, Accepted 23rd April 2012
DOI: 10.1039/c2cp24139k

Quasi-solid-state dye-sensitized solar cells have drawn the attention of scientists and technologists as a potential candidate to supplement future energy needs. The conduction of iodide ions in quasi-solid-state polymer electrolytes and the performance of dye sensitized solar cells containing such electrolytes can be enhanced by incorporating iodides having appropriate cations. Gel-type electrolytes, based on PAN host polymers and mixture of salts tetrahexylammonium iodide ($Hex_4N^+I^-$) and MgI_2, were prepared by incorporating ethylene carbonate and propylene carbonate as plasticizers. The salt composition in the binary mixture was varied in order to optimize the performance of solar cells. The electrolyte containing 120% $Hex_4N^+I^-$ with respect to weight of PAN and without MgI_2 showed the highest conductivity out of the compositions studied, 2.5×10^{-3} S cm^{-1} at 25 °C, and a glass transition at −102.4 °C. However, the electrolyte containing 100% $Hex_4N^+I^-$ and 20% MgI_2 showed the best solar cell performance highlighting the influence of the cation on the performance of the cell. The predominantly ionic behaviour of the electrolytes was established from the dc polarization data and all the electrolytes exhibit iodide ion transport. Seven different solar cells were fabricated employing different electrolyte compositions. The best cell using the electrolyte with 100% $Hex_4N^+I^-$ and 20% MgI_2 with respect to PAN weight showed 3.5% energy conversion efficiency and 8.6 mA cm^{-2} short circuit current density.

1.0 Introduction

The development of renewable and clean energy sources is important in order to fulfill future energy needs without depleting our fossil fuels and without polluting our environment. Solar cells have been considered as an economical and convenient device for converting solar energy directly into electricity. In this regard, the utilization of solar energy is a well-deserved alternative. However, the high production cost of the conventional silicon solar cells is an obstacle to widespread utilization of solar energy. Hence, the low cost, dye sensitized solar cells (DSSCs) are emerging as a reliable alternative to fulfill future energy needs.[1–3] Another advantage of DSSCs is that they perform relatively better compared to other solar cell devices under diffuse light conditions and also at higher temperatures.[2] However, efficient, stable and robust DSSCs need to be developed in order to make them practically and commercially viable devices. In this regard, the improvement of the photo-electrode[4–8] and the electrolyte[9,10] is important to enhance the performance of DSSCs. In general, the overall energy conversation efficiency of a cell, light to electricity, is affected by many factors, including the catalyst used in the counter electrode,[11] the transmittance and the conductivity of the conducting substrate,[12,13] the electrolyte composition,[14] type of dye sensitizer,[15] and properties of the TiO_2 film.[4–8] The present study is primarily focused on improving the quasi-solid-state or gel polymer electrolyte for DSSCs due to many favorable characteristics of such electrolytes over liquid type electrolyte based devices.

The most commonly used liquid electrolyte in DSSCs is the iodide/triiodide redox couple in liquid organic solvents such as acetonitrile and propylene carbonate (PC), with this electrolyte a high overall energy conversion efficiency of more than 10%[3,15–17] has been recorded for small area cells. However, to develop practicable large area and chemically and physically stable solar cells, the use of a liquid type electrolyte is a major drawback.

[a] *Department of Applied Physics, Chalmers University of Technology, Gothenburg, Sweden. E-mail: awijendr@yahoo.com*
[b] *Department of Physical Sciences, Rajarata University of Sri Lanka, Sri Lanka*
[c] *Institute of Fundamental Studies, Hantana Road, Kandy, Sri Lanka*
[d] *Postgraduate Institute of Science, University of Peradeniya, Sri Lanka*
[e] *Department of Physics, University of Gothenburg, Gothenburg, Sweden*

Hence, replacing the liquid electrolyte by a solid or a quasi-solid-state polymer electrolyte is an important strategy for fabricating practically and commercially viable DSSCs.[9,18,19]

Polymer electrolytes introduced in the 1970s consist of an appropriate salt dissolved in a polymer matrix signifying a unique class of electrolytes. They are very attractive materials to be used in applications such as batteries, photo electrochemical (PEC) solar cells, electro-chromic devices, supercapacitors and fuel cells due to the favorable mechanical properties, ease of fabrication and minimum side reactions.[20,21] However, the major disadvantage of solid-polymer electrolytes is their low ionic conductivity compared to liquid-type electrolytes[22,23] leading to low efficiencies in the abovementioned devices. However, polyacrylonitrile (PAN) based quasi-solid polymers or gel electrolytes have been reported to have reasonably good ionic conductivities and they have been used in quasi solid-state PEC solar cells.[9,18,24] Development of gel polymer electrolytes with high iodide-ion conductivity is important in order to improve the efficiency and finally to fabricate commercially viable DSSCs since the iodide/triiodide redox couple has been the mostly used redox couple for DSSCs so far.[2,3] Very recently incorporation of $Co^{(II/III)}$ tris(bipyridyl) redox couple in an electrolyte has shown better efficiencies with porphyrin-sensitized DSSCs.[25] However, for the mostly used ruthenium based dye complexes the best reported electrolytes contain iodide/triiodide redox couples.[2,3,17,29]

In order to develop quasi-solid or solid polymer electrolytes intended for PEC solar cells, various host polymers and plasticizers have been incorporated with different iodide salts.[2,9,18,24] The nature of the cation in the iodide salt incorporated with the host polymer matrix plays an important role in the ion transport mechanism in DSSCs. The incorporation of different alkaline metal iodides in PAN based[26] and (polyethylene oxide) PEO based[27] polymer electrolytes for PEC solar cells has been reported. The study on electrolytes containing PAN has suggested that the short circuit photocurrent density (J_{SC}) enhances more or less with increasing size of the cation.[26] Studies of PEO based gel polymer electrolytes with different alkyl metal iodides have shown that there is a conductivity enhancement with increasing cation size for all salts except for CsI.[27] The application of these electrolytes in DSSCs reveals a clear improvement of the open circuit voltage with the size of the cation. Conversely, iodides having small cations have shown better short circuit current densities in some cases.[27] However, in general it is evident that the iodide ion conductivity in solid/gel polymer electrolytes and the performance of DSSCs containing such an electrolyte can be enhanced by incorporating salts containing bulky cations such as quaternary-ammonium iodides and ionic liquids.[9,10,18,24]

When the size of the cation increases it enhances the salt dissociation and anion transference number leading to high iodide ion conductivity which is important for improving the performance of the solar cell. For instance, tetrapropylammonium iodide ($Pr_4N^+I^-$) has been used with PEO and with PAN host polymers and reasonably good cell performance has been reported, reaching about 3% overall cell efficiency for PAN based electrolytes.[18,28] DSSCs containing PAN and tetrabutylammoniumiodide ($Bu_4N^+I^-$) salt have also been reported to show good cell performance.[24,29] In an earlier work by us, the use of tetrahexylammonium iodide ($Hex_4N^+I^-$) with PEO host polymers for electrolytes intended for all solid-state solar cells was reported together with a systematic study of the conductivity variation with the composition, however the cell efficiencies were low owing to low ionic conductivity of the electrolyte used.[22,30]

Apart from PAN, polyvinylidenefluoride (PVDF) based electrolytes have shown good solar cell performances. However, the best performing PVDF based electrolytes contain volatile solvents like acetonitrile[31] or acetone[32] and the reported highest efficiency is 7.3% according to our knowledge. However, PAN based electrolytes have also shown about 7.3% energy conversion efficiency even without using volatile solvents.[29] Most of the advantages that we expect replacing liquid electrolytes by gel electrolytes cannot be attained by electrolytes containing volatile solvents. Therefore in this work PAN is selected as a host polymer in order to improve solar cell performance.

The cation in the electrolyte semiconductor interface has profound influence on electron dynamics and hence the efficiency of DSSCs.[17,33] In a previous work by us two different PAN based quasi-solid electrolyte systems were investigated using $Hex_4N^+I^-$[34] and MgI_2[9] salts and the conductivity was systematically optimized by varying compositions and the high iodide ion conducting electrolytes obtained were used successfully in DSSCs. However, some recent research has shown that quasi-solid electrolyte complexes with salt mixtures give better DSSC performances[35,36] for quasi-solid-state DSSCs. This can be understood by studying the effects of the cations on the charge injection mechanism at the electrolyte interface to the dye coated TiO_2 film and electron transport to the conducting tin oxide (CTO) through the TiO_2 film. Kelly *et al.* studied the influence of cations on the excited-state deactivation kinetics of a dye coated TiO_2.[37] They have shown that the magnitude of electron injection yields of the dye varies with the charge-to-radius ratio of the cation in the electrolyte, with $Ca^{2+} > Sr^{2+} \sim Ba^{2+} > Li^+ > Na^+ > K^+ = Rb^+ \sim Cs^+ \sim Bu_4N^+I^-$. The transport of injected electrons to the CTO substrate is described using a diffusion mechanism. However, the reported diffusion coefficient for DSSCs with porous TiO_2 film is low compared to that of single crystal TiO_2 due to the presence of electron trapping sites in porous layers.[38,39] Therefore, the electron diffusion can be changed by cation adsorption or intercalation to the trapping sites. After analysis of diffusion coefficients using single salt liquid electrolytes Kambe *et al.* expected to have higher diffusion and favourable photo-generation of electrons in cells having electrolytes containing a double cationic system.[38] In another study of DSSCs containing aqueous electrolyte with various cations it was shown that the short circuit current density increases with increasing charge density of the cation in the electrolyte while the fill factor, open circuit voltage and efficiency decrease.[40] Conversely, the bulky cations improve the iodide ion conductivity in quasi-solid-state polymer electrolytes. The aim of the present work is to optimise the ionic conductivity systematically by means of varying the $Hex_4N^+I^-$ and MgI_2 salt composition in a PAN based electrolyte and to investigate thermal and transport properties in order to find reliable and efficient electrolytes

for DSSCs and to understand the effects of the cations in the electrolyte for the cell performance.

2.0 Experimental

PAN, $Hex_4N^+I^-$, iodine, propylene carbonate (PC) and ethylene carbonate (EC) all with purity greater than 98%, purchased from Aldrich, were used as starting materials. PAN and $Hex_4N^+I^-$ were vacuum dried for 24 hours in a vacuum oven at 50 °C prior to use. For preparing the electrolyte samples the weights of PAN (0.1 g), EC (0.4 g) and PC (0.4 g) were kept unchanged and the weights of $Hex_4N^+I^-$ and MgI_2 were varied as given in Table 1. The weight of iodine in the electrolyte was maintained so that the molar ratio of salt : I_2 is 10 : 1. For preparing the electrolyte samples, initially the relevant weights of EC, PC and salts were mixed in a closed glass bottle by continuous stirring at 50 °C for about 3 hours. Then PAN was added to the mixture which was stirred further keeping it at 40 °C for about 2 hours. Finally, iodine was added to the mixture and heated to about 100 °C along with continuous stirring for a few more minutes until a homogeneous viscous solution was obtained. When the MgI_2 amount is increased a more viscous gel was obtained making the stirring more difficult. The resulting slurry was then cast onto a glass plate and pressed by another glass plate in order to obtain a quasi-solid-state polymer electrolyte film.

The complex impedance measurements were performed using a HP 4292A RF impedance analyzer in the frequency range of 10 Hz–10 MHz and in the temperature range of 0 °C to 60 °C. Disc shaped electrolyte films of diameter 10.5 mm and thickness about 0.8 mm, sandwiched between two polished stainless steel blocking electrodes, were used for impedance measurements.

DC polarization tests were carried out at room temperature by sandwiching a disc shaped electrolyte sample between two stainless steel blocking electrodes (SS) or between two iodine non-blocking electrodes, the configurations were thus SS–electrolyte–SS or SS–I_2–electrolyte–I_2–SS. The thermal properties of the samples were analyzed using a Mettler Toledo DSC 30 differential scanning calorimeter between −140 °C and 100 °C in consequent heating and cooling cycles, with a rate of 10 °C min^{-1}. The same sample was scanned few times subsequently in order to obtain data for 2nd, 3rd and 4th heating runs.

A TiO_2 nano-porous layer was coated on fluorine-doped tin oxide (FTO) glass using Degussa P25 powder. For this layer preparation, 0.5 g of Degussa powder (TiO_2) was ground well for ~30 minutes with ~2 ml of HNO_3 (pH = 1) in an agate mortar.

Table 1 Electrolyte compositions, where the weights of PAN, EC and PC were kept at 0.10 g, 0.40 g and 0.40 g respectively

Electrolyte	MgI_2/g	$Hex_4N^+I^-$/g	I_2/mg	Weight ratio PAN : $[Hex_4N^+I^-]$: $[MgI_2]$
a	0.12	0.00	10.9	100 : 0 : 120
b	0.10	0.02	10.2	100 : 20 : 100
c	0.08	0.04	9.4	100 : 40 : 80
d	0.06	0.06	8.6	100 : 60 : 60
e	0.04	0.08	7.8	100 : 80 : 40
f	0.02	0.10	7.1	100 : 100 : 20
g	0.00	0.12	6.3	100 : 120 : 0

The resulting colloidal suspension was diluted to get a 5% (w/w) solution and subsequently, it was stirred overnight at 60 °C and 25% (w/w) solution was obtained. Then ~0.1 g of carbowax and few drops of Triton X 100 (surfactant) were added and mixed well. This colloidal suspension was cast using a doctor blade method for obtaining porous TiO_2 layers of about 5–10 μm thickness after sintering at ~450 °C for 30 min. The TiO_2 coated electrodes were immersed in an ethanolic solution of dye sensitizer ruthenium 535-bis TBA (Solaronix SA) while both were hot (~60 °C). After 24 h absorption, the electrode was withdrawn from the dye solution and washed with acetone to remove unabsorbed dye and loosely bound TiO_2 particles in the dye-coated electrode.

Quasi solid-state PEC solar cells were fabricated by sandwiching polymer electrolyte films of thickness about 0.1–0.5 mm between the dye-coated TiO_2 electrode and a Pt coated glass (mirror type) electrode in the configuration glass–FTO–dye-TiO_2–electrolyte–Pt–FTO–glass. All the fabricated solar cells were characterized by measuring *I–V* curves using a computer controlled eDAQ Potentiostat and e-coder under the ~1000 W m^{-2} irradiation (1.5 AM) with a LOT-Oriel GmbH solar simulator using an 11 mm^2 slit.

3.0 Results and discussion

3.1 Ionic conductivity

From the nature of the PAN/EC/PC:MgI_2/$Hex_4N^+I^-$ polymer electrolyte complexes, fabricated according to compositions given in Table 1, they cannot be classified as solid-state electrolytes, but can be defined as quasi-solid or gel or rubbery type. In order to obtain free standing film, the thickness must be at least 0.4 mm. A picture of a 0.5 mm thick electrolyte sample is shown in Fig. 1. However, samples with more MgI_2 are shown to be apparently more solid in nature, which can be due to the cross linking of polymer chains by small Mg^{+2} ions. Fig. 2a shows the conductivity variation as a function of inverse temperature of these quasi-solid-state electrolyte samples for different salt compositions with respect to the weight of PAN in the electrolyte (expressed as wt% with respect to PAN weight as given in column 5 in Table 1). The conductivity of the electrolyte containing only MgI_2 as salt (sample a) is low,

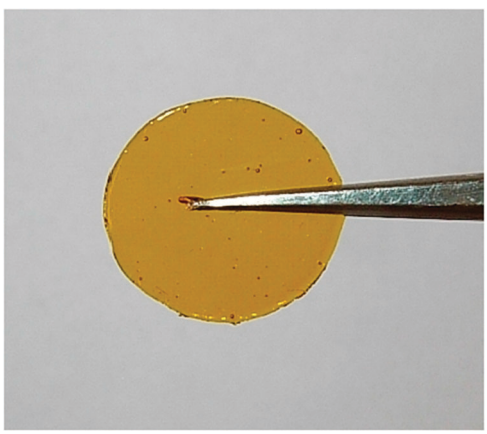

Fig. 1 A picture of a 0.5 mm thick, free standing gel electrolyte sample.

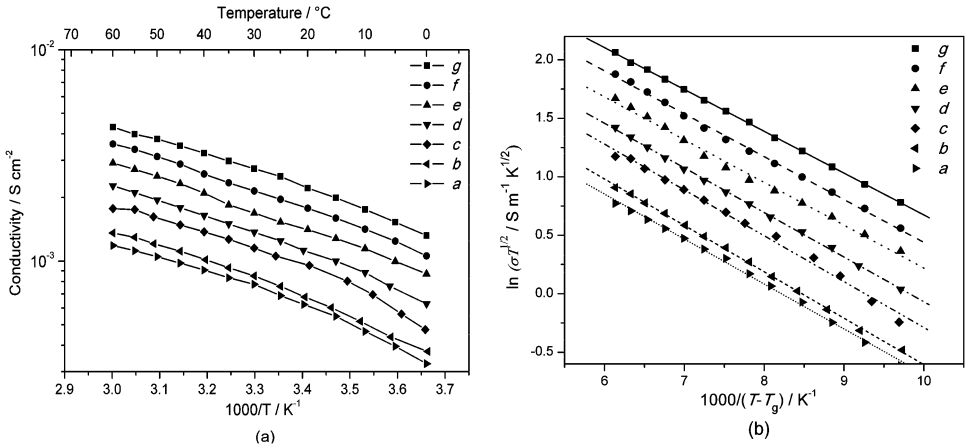

Fig. 2 (a) σ *versus* $1000/T$ for PAN/EC/PC:$Hex_4N^+I^-$:MgI_2 electrolytes containing different $Hex_4N^+I^-$ and MgI_2 compositions. (b) $\ln(\sigma T^{1/2})$ *vs.* $1000/(T - T_g)$ for PAN/EC/PC:$Hex_4N^+I^-$:MgI_2 electrolytes containing different $Hex_4N^+I^-$ and MgI_2 compositions as given in Table 1. Fitted lines to the VTF equation are also shown.

for instance 6.86×10^{-4} S cm^{-1} at 25 °C and 1.05×10^{-3} S cm^{-1} at 50 °C. The conductivity gradually increases with the increasing amount of $Hex_4N^+I^-$ in the electrolyte. Consequently, the electrolyte containing only $Hex_4N^+I^-$ salt (sample g) shows the highest conductivity, 2.51×10^{-3} and 3.78×10^{-3} S cm^{-1} at 25 °C and 50 °C respectively.

The conductivity (σ) variations of all electrolytes show Vogel–Tammann–Fulcher (VTF) behaviour and were fitted to the VTF equation

$$\sigma = AT^{-1/2}\exp\left(-\frac{E_a}{k_B(T - T_o)}\right) \quad (1)$$

where σ is the conductivity, T is the absolute temperature, A is a pre-exponential factor, E_a is the pseudo activation energy and T_o is the reference temperature which is related to the equilibrium state glass transition temperature.[41] In this work the measured glass transition temperature, T_g, was employed as the reference temperature T_o for fitting and the appropriateness of the selected T_g is justified by the good fitting shown in Fig. 2b within the measured temperature range. A and E_a values obtained by fitting conductivity data to eqn (1) are given in Table 2. E_a values fluctuate at around 30 meV, lower activation energies are observed when the electrolyte conductivity is high, except for sample g. In general, the pre-exponential factor, A, is proportional to the number of ionic charge carriers in the electrolyte and E_a reveals the energy characteristics.[41] As shown in Table 2, A increases as the amount of $Hex_4N^+I^-$ increases, suggesting that the number of ionic charge carriers increases with increasing amount of $Hex_4N^+I^-$. The reason may be the higher degree of salt dissociation due to lower lattice energy of $Hex_4N^+I^-$ compared to MgI_2.[22]

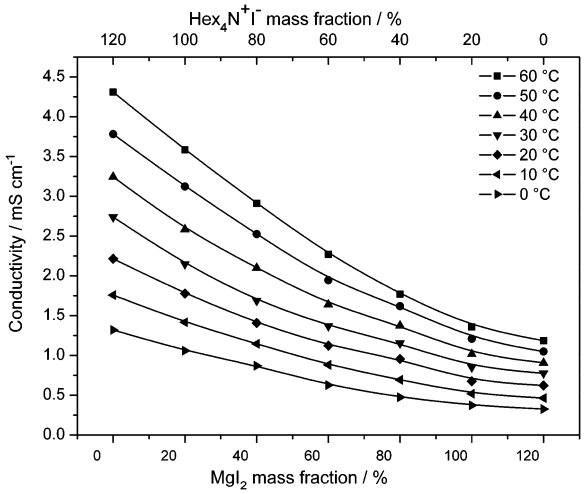

Fig. 3 Conductivity as a function of $Hex_4N^+I^-$ and MgI_2 salt mass fractions with respect to PAN in PAN/EC/PC:$Hex_4N^+I^-$:MgI_2 electrolyte at different temperatures.

Fig. 3 shows the variation of ionic conductivity as a function of the mass fraction of the salt (x%) with respect to PAN at temperatures 0, 10, 20, 30, 40, 50 and 60 °C. The conductivity increases with increasing temperature, as expected since the ion transport and salt dissociation increase with increasing temperature besides the reduction of local viscosity. However, a conductivity reduction is shown with the increase in MgI_2 salt composition. Therefore, increasing amounts of MgI_2 may have reduced the polymer flexibility *via* strong cross linking of long polymer chains reducing the mobility of ions, since the high charge density in the small Mg^{+2} cation assists the cross

Table 2 The activation energy, E_a, pre-exponential factor, A, and the glass transition temperature, T_g, for electrolytes containing different mass fractions of MgI_2 and Hex_4NI

Sample	a	b	c	d	e	f	g
[$Hex_4N^+I^-$] : [MgI_2] weight ratio	0 : 120	20 : 100	40 : 80	60 : 60	80 : 40	100 : 20	120 : 0
E_a/meV	33.1	34.2	33.8	32.8	31.6	31.5	30.8
A/S m^{-1} K$^{1/2}$	23.5	28.8	37.8	42.3	48.4	60.7	70.1
T_g/°C	−102.4	−104.5	−103.5	−103.6	−103.6	−103.8	−102.4

linking of PAN chains due to the presence of a CN group in the polymer. In a previous work by us this cross linking ability of Mg^{+2} was used to improve the iodide ion transport number in a PAN based electrolyte system.[9] In contrast to the effect of MgI_2, a conductivity increase is shown with the increase in $Hex_4N^+I^-$ salt composition in this PAN/EC/PC:MgI_2/$Hex_4N^+I^-$ electrolyte. This conductivity increase with increasing $Hex_4N^+I^-$ mass fraction can be attributed basically to an increase in both the number of charge carriers and their mobility with added $Hex_4N^+I^-$. A higher salt dissociation can be due to the reduction of lattice energy of the salt caused by the presence of bulky cations in the $Hex_4N^+I^-$ salt.[22] The higher salt dissociation with increasing amount of $Hex_4N^+I^-$ is evident from the increase in the pre-exponential factor, A, which correlates with the density of charge carriers as given in Table 2.[41] In addition, this bulky cation can impose more disorder on long polymer chains and it can make long polymer chains more separated increasing the flexibility of the material. Finally, the $Hex_4N^+I^-$ salt has given a significant ionic conductivity enhancement compared to MgI_2.

3.2 DSC measurements

Fig. 4 shows the differential scanning calorimetric (DSC) thermograms of PAN/EC/PC:$Hex_4N^+I^-$/MgI_2 electrolyte samples with different $Hex_4N^+I^-$ and MgI_2 mass fractions for the 2nd heating run. There were minor dissimilarities between DSC thermograms obtained during the 1st and the 2nd heating runs. When comparing the 2nd, 3rd and 4th runs such dissimilarities were not observed. The measurements of samples obtained during the 2nd cycle were selected for this study in order to eliminate effects of thermal history. A clear glass transition at around −100 °C can be observed for all samples. The glass transition temperatures, T_g (mid-point), obtained using the 2nd heating cycle are given in Table 2. The glass transition at around −100 °C has been reported in the literature for PAN/EC/PC electrolytes for other comparable systems.[9] These measured T_g values were used in the VTF equation as mentioned earlier.

The T_g result can be related to a change in the segmental flexibility of polymeric chains of the electrolyte due to the incorporation of the salt[42,43] and also through the flexibility to the mobility of charge carriers.[44] Low T_g values were observed for the electrolyte containing salt mixtures since more structural disorder can be induced by salt mixtures containing ions with different size and charge. The highest T_g is observed and minimum conductivity was shown for the electrolyte containing only the MgI_2 salt (sample a). However, the conductivity increase shown in Fig. 3 with added $Hex_4N^+I^-$ is mainly caused by the increasing number of charge carriers with added $Hex_4N^+I^-$ since the T_g remains essentially unchanged over the entire composition range. In general, a liquid-like charge transport mechanism where the electrolyte solution is trapped in cages formed by the PAN matrix has been suggested for this type of PAN based electrolytes.[29,45]

3.3 DC polarization measurements

Results of DC polarization measurements[46] obtained for all the electrolyte compositions are given in Table 1, the measurements were performed using 1.0 V bias voltage and at 25 °C, the data obtained for samples a and f are shown in Fig. 5. When stainless steel (SS) electrodes were used in SS–electrolyte–SS blocking electrode configuration, an abrupt current drop is observed within the first 10 minutes, the current then reached a more or less stable value after about 60 minutes.[47] Hence, these electrolytes show a predominantly ionic nature (more than 90%). Polarization measurements in the SS–I_2–electrolyte–I_2–SS symmetrical non-blocking configuration showed no appreciable current drop during the measurement time period. Similar DC polarization results were obtained for all other salt compositions. This ensures that all electrolytes tested are predominantly iodide ion conductors. Therefore, the transference number of the cation in this system can be estimated to be less than 10%, evidently as a result of the large size of the $Hex_4N^+I^-$ cation. On the other hand the transport of Mg^{+2} in the electrolyte is also very small compared to the iodide ion transport number. High iodide ion conductivity makes these

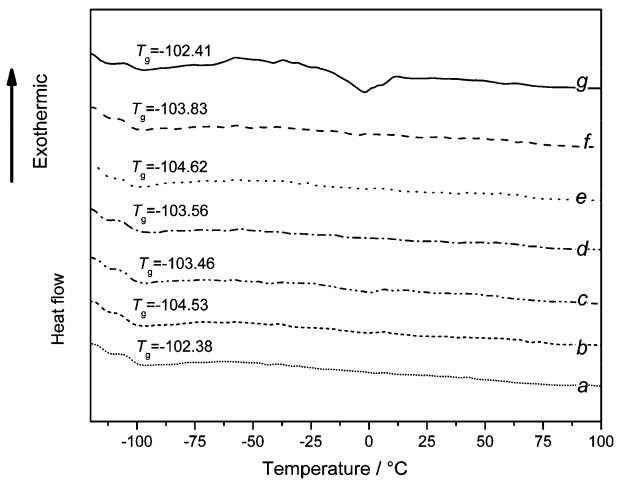

Fig. 4 DSC thermograms of PAN/EC/PC polymer electrolytes containing different weights of $Hex_4N^+I^-$ and MgI_2 with respect to PAN weight under a heating rate of 10 °C min^{-1}. The composition of samples a,b,...g is given in Table 1.

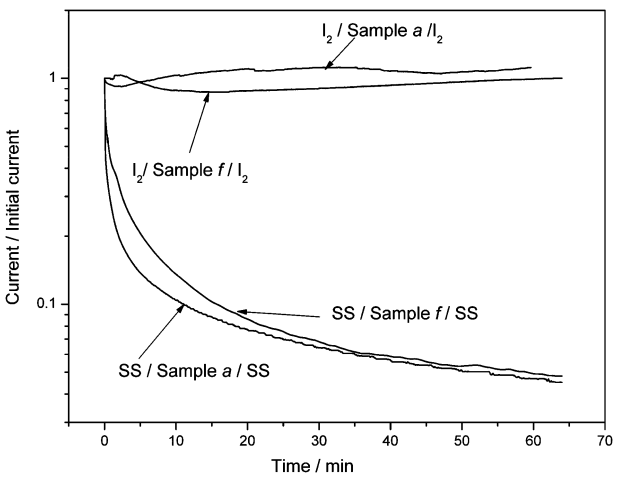

Fig. 5 Current/initial current *vs.* time plot for two PAN/EC/PC:$Hex_4N^+I^-$:MgI_2 electrolyte samples given in Table 1 taken from DC polarization measurements at 25 °C. Curves correspond to the SS–electrolyte–SS and SS–I_2–electrolyte–I_2–SS configurations as marked.

electrolytes an ideal candidate for TiO_2 based DSSCs and other electrochemical applications.

3.4 Solar cell characterization

The *V–I* characteristic curves for cells fabricated using PAN based quasi-solid electrolytes containing different $Hex_4N^+I^-$ and MgI_2 compositions are shown in Fig. 6 at room temperature. The inset shows the efficiency and short-circuit-current density variation with MgI_2 mass fraction with respect to PAN. Seven different cells were fabricated employing seven different electrolyte compositions. The short-circuit photocurrent density (J_{SC}) and open-circuit voltage (V_{OC}) under the irradiation of 1000 W m^{-2} of each of the cells are shown in Table 3. The fill factor, ff, was calculated using

$$\mathrm{ff} = \frac{J_{opt} V_{opt}}{J_{SC} V_{OC}} \qquad (2)$$

where J_{opt} and V_{opt} are the current density and voltage at maximum power output. The fill factor and the energy conversion efficiency, η, are also included in Table 3 for all cells. The η is calculated using

$$\eta = \frac{J_{SC} V_{OC} \mathrm{ff}}{\text{Total incident power density}} \qquad (3)$$

All cells exhibited energy conversion efficiencies of more than 2%. The best energy conversion efficiency is shown by the cell that contains electrolyte sample f which consists of 20% MgI_2 and 100% $Hex_4N^+I^-$ with respect to PAN weight. Even though electrolyte g which contains 120% $Hex_4N^+I^-$ and no MgI_2 shows the best conductivity, the efficiency of the cell with electrolyte sample g is lower than that of the cell with electrolyte sample f. This behaviour can be understood by

Table 3 The performance of DSSCs prepared using electrolytes containing different MgI_2 and $Hex_4N^+I^-$ compositions given in Table 1. Efficiency measurements could be repeated within 0.2 percentage units

Electrolyte	J_{sc}/ mA cm^{-2}	V_{oc}/ mV	J_{opt}/ mA cm^{-2}	V_{opt}/ mV	ff/ %	Efficiency/ %
g	8.1	788.0	6.7	458.0	48.1	3.1
f	8.6	790.0	6.1	580.0	52.1	3.5
e	8.0	756.0	6.3	496.0	51.7	3.1
d	5.9	786.0	4.8	521.0	53.9	2.5
c	5.2	754.0	4.5	544.0	62.4	2.4
b	4.7	780.0	4.0	532.0	58.0	2.1
a	4.1	704.0	3.7	532.0	68.2	2.0

realizing the positive effects of incorporated small cations such as Mg^{++}, enhancement of electron injection yields from dye to TiO_2 film, electron diffusion through the TiO_2 layer, dye regeneration and effects imposed on the semiconductor band positions and negative effects like reduction of iodide ion conductivity with increasing amount of MgI_2.

For the optimum function of the DSSCs it is necessary that charges injected into the TiO_2 nano-particles should be screened on the mesoscopic scale by the surrounding electrolyte, facilitating electron percolation within the semiconductor towards the FTO.[39] The electron motion in the conduction band of the porous oxide film is coupled with an interfacial electron-transfer reaction and with ion transport within pores or in the interface. Hence the movement of electrons in the conduction band of the mesoscopic films is accompanied by the diffusion of charge-compensating cations in the electrolyte layer in the vicinity of the nano-particle surface. The cations screen the Coulomb potential of the electrons avoiding the formation of uncompensated local space charge.[39] Besides, it has been shown using

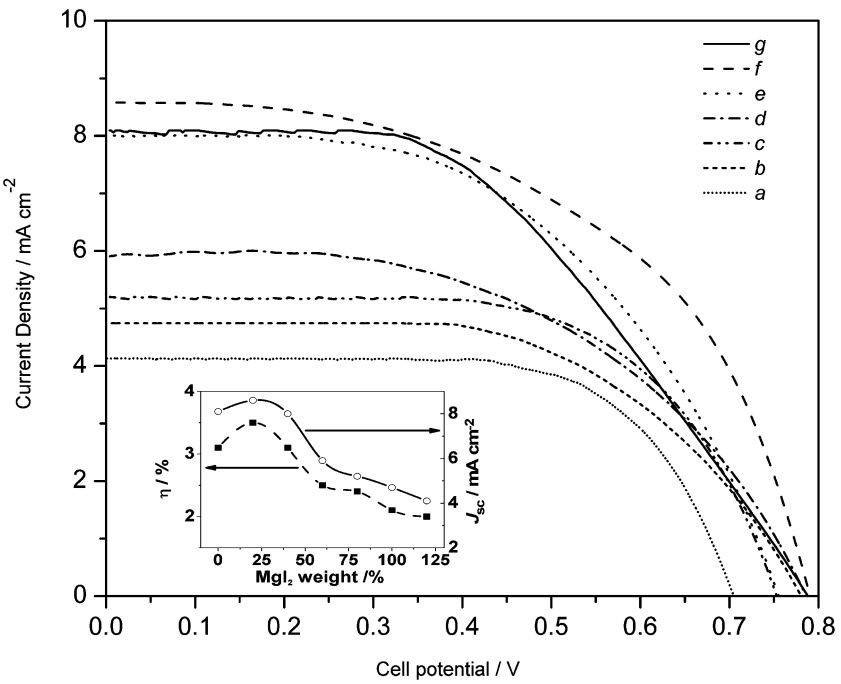

Fig. 6 Photocurrent *versus* cell potential for seven different DSSCs fabricated using PAN/EC/PC:MgI_2/$Hex_4N^+I^-$ electrolyte containing total of 120 wt% salts with respect to weight of PAN under irradiation of a 1000 W m^{-2} xenon lamp. The DSSCs are named using the electrolyte name given in Table 1. The scan time is 20 s. The inset shows the efficiency and short-circuit-current density variation with MgI_2 mass fraction.

electrophoresis measurements although that the bulky cation Bu_4N^+ cannot be adsorbed on the dye coated TiO_2 film, nevertheless Mg^{+2} ions do it very efficiently.[48] Since the size of the Hex_4N^+ ion is larger than that of Bu_4N^+ it can be inferred that the Hex_4N ion also cannot be adsorbed on the TiO_2 film. In addition, Kelly *et al*. have shown that adsorption of potential-determining cations on the TiO_2 surface is expected to have a strong effect on the electron injection rate and the resulting quantum yield in DSSCs.[37] In PEC solar cells, cation adsorption may alter surface charge, band edge positions, and the energy distribution of surface states. The cation behavior at the semiconductor–electrolyte interface is governed by electrostatics and surface adsorption. Cation adsorption would shifts the acceptor states in TiO_2 to more positive electrochemical potentials resulting in favourable energetics for interfacial charge injection.[37] Faster dye regeneration reaction is also highly important for the efficient performance of the DSSCs in particular reducing the back electron transfer.[33] It was reported that the reduction rate of the oxidized state of the dye strongly depends upon the nature of the cation and for instance the total recovery time for the oxidized dye is 4 μs and 40 μs in the presence of MgI_2 and $Bu_4N^+I^-$ respectively.[48]

Hence, the reported higher efficiency and J_{SC} for the cell in the presence of a small amount of Mg^{+2} ions in the electrolyte (sample f) can be clearly understood although electrolyte conductivity in this sample has decreased due to the presence of MgI_2. However, for the other tested electrolyte samples containing more than 40% MgI_2 the efficiency and J_{SC} decrease with the increasing amount of MgI_2 which can be correlated mainly with the drop in iodide ion conductivity in the electrolyte as shown in Fig. 3. These positive and negative competing processes, determined by the concentration of Mg^{+2} ions, have given rise to the observed variation in J_{SC} and V_{OC} and efficiency of the solar cells given in Table 3.

High iodide ion conductivity in the electrolyte is necessary for the better performance of quasi-solid-state DSSCs. On the other hand, the iodide ion conductivity is not the only factor governing the efficiency of the DSSCs since the cations in the electrolyte also have profound influence on the performance of the DSSCs. However, there are two competing factors. The iodide ion conductivity in the electrolyte increases with the increase in cation size whereas electron injection and charge separation in the photo-electrode have positive influence when the size of the cation decreases. Therefore, as seen from our results the electrolyte complex containing the mixed cations system gives better solar cell performance, compared to a single cation system. The highest J_{SC}, V_{OC} and efficiency of 790 mV, 8.6 mA cm^{-2} and 3.5 are shown for DSSC containing the electrolyte with 20% of MgI_2 and 100% of $Hex_4N^+I^-$.

4.0 Conclusions

Quasi solid-state polymer electrolytes, based on PAN host polymers, were prepared by incorporating the salts $Hex_4N^+I^-$ and MgI_2, and plasticizers EC and PC. The electrolyte containing a 120% salt mixture with respect to PAN weight showed the maximum conductivity out of the samples measured. This electrolyte membrane showed a conductivity of 2.51×10^{-3} S cm^{-1} and 3.78×10^{-3} S cm^{-1} at 25 °C and 50 °C, respectively, and a low T_g value of −102.4 °C. The predominantly ionic behaviour of the conductivity in the electrolyte was inferred from dc polarization data. In addition, cationic transport appears to be negligible and hence the dominant iodide ion transport would ensure the potential for using this PAN/EC/PC:Hex4N$^+$I$^-$/MgI_2 polymer electrolyte in TiO_2 based DSSCs. Seven different DSSCs were fabricated using different salt compositions in the electrolyte.

The electrolyte with the highest conductivity did not show the best energy conversion efficiency revealing that the effect of the cation on the efficiency of the DSSCs is equally important. The presence of a cation with high charge density in the electrolyte contributes to the performance enhancement of the DSSCs. The best cell result was an energy conversion efficiency of 3.5% and a short circuit current density of 8.6 mA cm^{-2}. It was shown that use of a mixed salt complex having cations with low and high charge densities can improve the efficiency of the DSSCs compared to having an electrolyte containing a single cation.

Acknowledgements

Research support from The National Research Council of Sri Lanka (grant 11-196), IPPS Uppsala as well as from the Swedish Research Council is gratefully acknowledged.

References

1 B. Li, L. Wang, B. Kang, P. Wang and Y. Qiu, *Sol. Energy Mater. Sol. Cells*, 2006, **90**(5), 549–573.
2 A. Hagfeldt, G. Boschloo, L. Sun, L. Kloo and H. Pettersson, *Chem. Rev*., 2010, **110**, 6595–6663.
3 Y. Chiba, A. Islam, Y. Watanabe, R. Komiya, N. Koide and L. Han, *Jpn. J. Appl. Phys*., 2006, **45**(25), L638–L640.
4 S. Ahmed, A. D. Pasquier, T. Asefa and D. P. Birnie III, *Adv. Energy Mater*., 2011, **1**, 879–887.
5 C. Y. Neo and J. Ouyang, *J. Power Sources*, 2011, **196**, 10538–10542.
6 M.-S. Wu, C.-H. Tsai, J.-J. Jow and T.-C. Wei, *Electrochim. Acta*, 2011, **56**, 8906–8911.
7 W.-J. Lin, C.-T. Hsu and Y.-C. Tsai, *J. Colloid Interface Sci*., 2011, **358**, 562–566.
8 B. Bills, M. Shanmugam and M. F. Baroughi, *Thin Solid Films*, 2011, **519**, 7803–7808.
9 T. M. W. J. Bandara, M. A. K. L. Dissanayake, I. Albinsson and B.-E. Mellander, *J. Power Sources*, 2010, **195**, 3730.
10 J. Wu, Z. Lan, D. Wang, S. Hao, J. Lin, Y. Huang, S. Yin and T. Sato, *Electrochim. Acta*, 2006, **51**, 4243.
11 X. Fang, T. Ma, G. Guan, M. Akiyama, T. Kida and E. Abe, *J. Electroanal. Chem*., 2004, **570**, 257.
12 N. J. Podraza, C. Chen, D. Sainju, O. Ezekoye, M. W. Horn, C. R. Wronski and R. W. Collins, Thin-Film Compound Semiconductor Photovoltaics, *Mater. Res. Soc. Symp. Proc*., 2005, **865**, 273.
13 W. J. Lee, E. Ramasamy, D. Y. Lee, B. K. Min and J. S. Song, Photonics: Design, Technology and Packaging II, *Proc. SPIE-Int. Soc. Opt. Eng*., 2006, **6038**, 413.
14 K. Hara, T. Nishikawa, M. Kurashige, H. Kawauchi, T. Kashima, K. Sayama, K. Aika and H. Arakawa, *Sol. Energy Mater. Sol. Cells*, 2005, **85**, 21.
15 M. K. Nazeeruddin, P. Pechy, T. Renouard, S. M. Zakeeruddin, R. Humphry-Baker, P. Comte, P. Liska, L. Cevey, E. Costa, V. Shklover, L. Spiccia, G. B. Deacon, C. A. Bignozzi and M. Graetzel, *J. Am. Chem. Soc*., 2001, **123**, 1613.
16 L. Han, N. Koide, Y. Chiba, A. Islam, R. Komiya, N. Fuke, A. Fukui and R. Yamanaka, *Appl. Phys. Lett*., 2005, **86**, 213501.
17 B. O'Regan and M. Grätzel, *Nature*, 1991, **353**, 737.

18 O. A. Ileperuma, M. A. K. L. Dissanayake, S. Somasunderam and L. R. A. K. Bandara, *Sol. Energy Mater. Sol. Cells*, 2004, **84**, 117.
19 J. Gong, K. Sumathy and J. Liang, *Renewable Energy*, 2012, **39**, 419–423.
20 M. B. Armand, M. J. Chabagno and M. J. Duclot, in *Fast ion transport in solids*, ed. P. Vashishta, J. N. Mandy and G. K. Shenoy, Elsevier North Holland, New York, 1979, pp. 131–136.
21 P. V. Wright, *Br. Polym. J.*, 1975, **7**, 319–327.
22 T. M. W. J. Bandara, P. Ekanayake, M. A. K. L. Dissanayake, I. Albinsson and B.-E. Mellander, *J. Solid State Electrochem.*, 2010, **14**, 1221–1226.
23 T. M. W. J. Bandara, M. A. K. L. Dissanayake, O. A. Ileperuma, K. Varaprathan, K. Vignarooban and B.-E. Mellander, *J. Solid State Electrochem.*, 2007, **12**, 913.
24 O. A. Ileperuma, G. R. A. Kumara and K. Murakami, *Chem. Lett.*, 2008, (1), 36–37.
25 A. Yella, H. Hsuan-Wei Lee, H. N. Tsao, C. Yi, A. K. Chandiran, M. K. Nazeeruddin, E. W.-G. Diau, C.-Y. Yeh, S. M. Zakeeruddin and M. Grätzel, *Science*, 2011, **334**, 629.
26 K. Tennakone, G. K. R. Senadeera, V. P. S. Perera, I. R. M. Kottegoda and L. A. A. D. Silva, *Chem. Mater.*, 1999, **11**, 2474.
27 X. Shen, W. Xu, J. Xu, G. Liang, H. Yang and M. Yao, *Solid State Ionics*, 2008, **179**, 2027–2030.
28 M. A. K. L. Dissanayake, L. R. A. K. Bandara, R. S. P. Bokalawala, P. A. R. D. Jayathilaka, O. A. Ileperuma and S. Somasunderam, *Mater. Res. Bull.*, 2002, **37**, 867.
29 O. A. Ileperuma, G. R. A. Kumara, H.-S. Yang and K. Murakami, *J. Photochem. Photobiol., A*, 2011, **217**, 308–312.
30 T. M. W. J. Bandara, B.-E. Mellander and M. A. K. L. Dissanayake, *Solid State Ionics Fundamental Researches and Technological Applications*, *Proceedings of the 12th Asian Conference on Solid State Ionics*, ed. B. V. R. Chowdari, 2010, pp. 1066–1074.
31 K.-M. Lee, V. Suryanarayanan and K.-C. Ho, *J. Photochem. Photobiol., A*, 2009, **207**, 224–230.
32 A. R. Sathiya Priya, A. Subramania, Y.-S. Jung and K.-J. Kim, *Langmuir*, 2008, **24**(17), 9816–9819.
33 D. F. Watson and G. J. Meyer, *Coord. Chem. Rev.*, 2004, **248**, 1391–1406.
34 T. Svensson, T. M. W. J. Bandara, E. Lundell, I. Svensson, M. Furlani, I. Albinsson and B.-E. Mellander, Proceedings Solar Asia 2011 Int. Conf., Institute of Fundamental Studies, Kandy, Sri Lanka, 2011, 221–227.
35 S. Agarwala, C. K. N. Peh and G. W. Ho, *ACS Appl. Mater. Interfaces*, 2011, **3**, 2383–2391.
36 C.A. Thotawatthage, G.K.R. Senadeera, T.M.W.J. Bandara and M.A.K.L. Dissanayake, Proceedings of Solar Asia 2011 Int. Conf., Institute of Fundamental Studies, Kandy, Sri Lanka, 2011, 175–179.
37 C. A. Kelly, F. Farzad, D. W. Thompson, J. M. Stipkala and G. J. Meyer, *Langmuir*, 1999, **15**, 7047.
38 S. Kambe, S. Nakade, T. Kitamura, K. Wada and S. Yanagida, *J. Phys. Chem. B*, 2002, **106**, 2967–2972.
39 M. Gratzel, *Inorg. Chem.*, 2005, **44**(20), 6841–6851.
40 Y. Shi, Y. Wang, M. Zhang and X. Dong, *Phys. Chem. Chem. Phys.*, 2011, **13**, 14590–14597.
41 Y.-J. Wang, Y. Pan, L. Wang, M.-J. Pang and L. Chen, *J. Appl. Polym. Sci.*, 2006, **102**, 4269–4275.
42 Y. Tominaga, S. Asai, M. Sumita, S. Panero and B. Scrosati, *J. Power Sources*, 2005, **146**, 402.
43 Y.-J. Wang, Y. Pan, L. Wang, M.-J. Pang and L. Chen, *Mater. Lett.*, 2005, **59**, 3021.
44 S. Zhang, S. Dou, R. H. Colby and J. Runt, *J. Non-Cryst. Solids*, 2005, **351**, 2825.
45 P. A. R. D. Jayathilaka, M. A. K. L. Dissanayake, I. Albinsson and B.-E. Mellander, *Solid State Ionics*, 2003, **156**, 179–195.
46 M. Watanabe, S. Nagano, K. Sanui and N. Ogata, *Solid State Ionics*, 1988, **911**, 28–30.
47 O. A. Ileperuma, M. A. K. L. Dissanayake and S. Somasundaram, *Electrochim. Acta*, 2002, **47**, 2801–2807.
48 S. Pelet, J. E. Moser and M. Gratzel, *J. Phys. Chem. B*, 2000, **104**, 1791.